DAS applications for near-surface characterization and traffic conditions assessment

Raul Cova, Heather K. Hardeman-Vooys, Da Li and Matt McDonald

ABSTRACT

Using distributed acoustic sensing (DAS), previously deployed telecommunication optical fibres can be repurposed as permanent seismic sensors. The ability of this system to acquire data for large distances (>10 km) and with a dense sampling (<1 m) makes this technology very attractive for near-surface monitoring and characterization. We show two applications that illustrate the potential of DAS data for these purposes. First, by using interferometric principles, we compute virtual source gathers from the ambient noise recorded by the fibre. This process allowed us to reconstruct the surface-wave propagation that would have been recorded between two different points along the fibre simulating an active source experiment. Then, dispersion spectra were computed from the data showing the ability of the DAS data to provide the necessary input for near-surface characterization methods like MASW (multichannel analysis of surface waves). A second application of DAS is explored using data acquired along the Ctrain tracks in the City of Calgary. From the raw data, it is possible to identify the signature of different sources propagating with different apparent velocities. Here, we compute the velocities of these signals by using a series of windowed τ-p transformations. Assuming that most of these signals are generated by vehicles driving along the roads next to the Ctrain tracks, this information can be used for monitoring traffic condition in terms of the velocity of the vehicles recorded at any time of the day. We also compute spatial average velocities, vehicle density and estimated travel times that can be used to interpret changes in traffic conditions throughout the day in a given section of the road.

INTRODUCTION

The ability of distributed acoustic sensing systems to record data permanently and over large distances has made of it a very common choice for measuring changes in environmental parameters induced by multiple events. A variety of applications can be found in the literature including safety and integrity monitoring applications in diverse sectors including transportation, oil and gas and process control systems. Also, the compatibility to optical fibre communication systems has allowed the repurposing of many kilometers of fibre already deployed to be used as permanent acoustic sensors.

For geophysicists in particular, DAS technology has provided access to spatially dense measurements of strain changes produced by the propagation of seismic waves. This has enabled multiple applications including the acquisition of vertical seismic profiles (VSP), microseismic measurements, well and reservoir surveillance, hydraulic fracturing monitoring and diagnostics.

Here, we show two potential applications of DAS data that were explored during the Industrial Problem Solving Workshop 2018 organized by the Pacific Institute for the Mathematical Sciences. First we show how to compute a surface-wave dispersion spectrum using

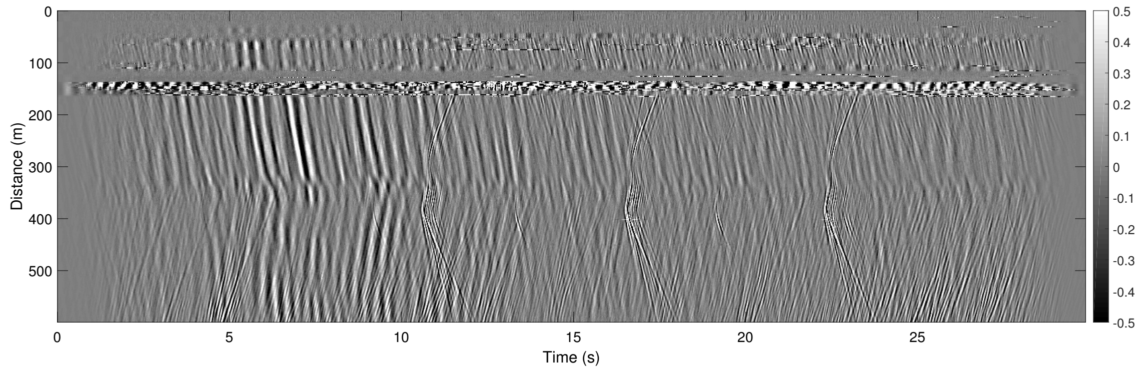

FIG. 1. Input DAS data.

DAS data. This spectrum is the main input for computing S-wave velocities in the near-surface that can be used to characterize soil conditions. The second application consists of using DAS data for monitoring traffic condition along a highway. This could provide useful information for city planning and roads condition monitoring in real time.

DISPERSION SPECTRA FROM DAS DATA

Claerbout (1968), Lobkis and Weaver (2001), and Wapenaar (2004), among other authors, have shown how the Green's function between two stations can be empirically estimated using the crosscorrelation of diffuse wavefields (e.g. ambient noise, scattered coda waves). Schuster et al. (2004) developed a theory were the random condition of the source locations initially proposed by Claerbout is relaxed enabling the application of these concepts to active seismic data. Shapiro and Campillo (2004) sets the foundation for the application of these concepts using ambient noise. More recently, Dou et al. (2017) and Zeng et al. (2017) applied ambient noise interferometry using DAS data to compute surface-wave dispersion spectra. In these studies, seismic records of several hours and even days are used to produce the desired dispersion spectrum.

Here we used DAS data recorded from an optical fibre buried next to a road. The data was acquired with a channel spacing of 0.67 m and frequency sampling of 20 kHz. The maximum record length we used for this experiment was 30 s. Figure 1 shows the data recorded over a segment of 600 m. Surface-waves are exited by a person standing next to the fibre and dropping a rock. These are the events observed at 11 s, 17 s and 23 s in the record in Figure 1. There we can see that the source is located close the channel located at 400 m from the origin of the segment.

We follow the workflow detailed in Bensen et al. (2007) to compute a dispersion spectrum using interferometric principles. First, the data in Figure 1 is split in windows of 4 s. Then, amplitudes are gained using an automatic gain process with a window length of 1 s. Next, the spectrum of the data is whitened by using a frequency domain deconvolution. In this process, the amplitude spectrum of each trace is smoothed using a 15 points Gaussian smoother and its inverse is used as the deconvolution operator. The left panels from Figure 2a to Figure 2g show the seven data windows after amplitude balancing and deconvolution.

A virtual source gather was then created by taking the first trace in each window and crosscorrelating it with the rest of the traces in the data panel. The middle column in Figure 2 shows the central part of the crosscorrelations between the time lags -2 s and 2 s. Notice that the effect of the crosscorrelation is that of subtracting the traveltimes between the reference trace and each trace in the panel. This provides the traveltimes that would have been recorded if an active source had been fired at the location of the channel used as the reference source. This output is accumulated and stacked with the output of the previous data windows. The panels at the right in Figure 2 show how the virtual source gather is progressively constructed as the crosscorrelation outputs are stacked. The integration allows the attenuation of random noise and the reinforcement of the coherent part of the signal present in each window. Linear events with low frequency content, characteristics of surface-wave propagation, can be identified between 0 s and 0.7 s. More importantly, as the data is integrated the dispersive character of these events becomes more evident.

Figures 3a and 3b show the final virtual source gather and its corresponding dispersion spectrum, respectively. The dispersion spectrum was computed by first applying a linear τ-p transformation covering the phase velocities between 0 m/s and 800 m/s. Then, we apply a Fourier transform along the τ axis and compute its absolute value. Finally, the slowness values p are converted into velocities and then data are interpolated into a regular grid of velocity and frequency values.

In Figure 3b, it is possible to interpret two surface-wave modes. The fundamental mode is represented by the area of maximum energy with the lowest frequency content (4 Hz to 12 Hz). Then, the first higher mode can be identified between 12 Hz and 25 Hz with phase velocities between 280 m/s and 320 m/s.

The areas of high energy in the dispersion spectrum can be picked to create dispersion curves. These curves can be used as an input for computing near-surface S-wave velocity profiles using techniques like the multichannel analysis of surface-waves (Park et al., 1999). The inversion process needed to accomplish this goal was beyond the scope of this experiment and it will be explored in future studies.

Assessing traffic conditions from DAS data

Advances in information and communication technologies applied to transportation and traffic management systems have led to the development of Intelligent Transportation Systems (ITS). Their main goal is to improve safety, efficiency, and sustainability of transportation networks. Proper management of these systems can have an enormous economical and environmental impact by reducing traffic congestion and enhancing drivers' experiences. To accomplish this goal, traffic management systems are required to provide accurate estimations of traffic parameters such as average vehicle speed and density. They also must be cost-effective for large scale deployments and maintenance and they must operate in all weather day-night conditions (Barbagli et al., 2012). DAS measurements can provide part of the critical data needed for ITS to accomplish their goal. Moreover, the ability to repurpose communication optical fibres can significantly reduce the costs of deployment and maintenance of a DAS-based ITS.

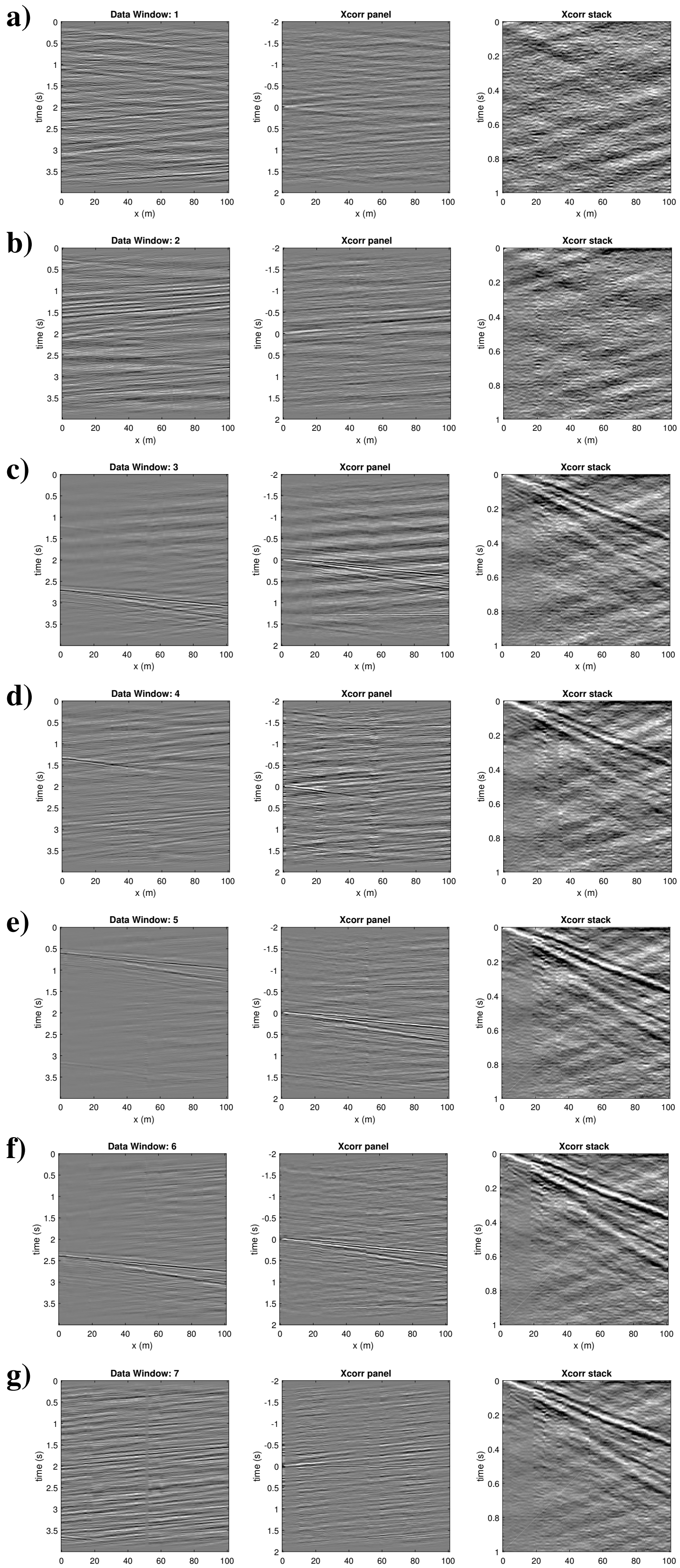

FIG. 2. Left column: data windows used for generating a virtual source gather. Middle column: crosscorrelation between the reference trace ($X = 0$ m) and all the other traces in the window. Right column: accumulated crosscorrelation functions.

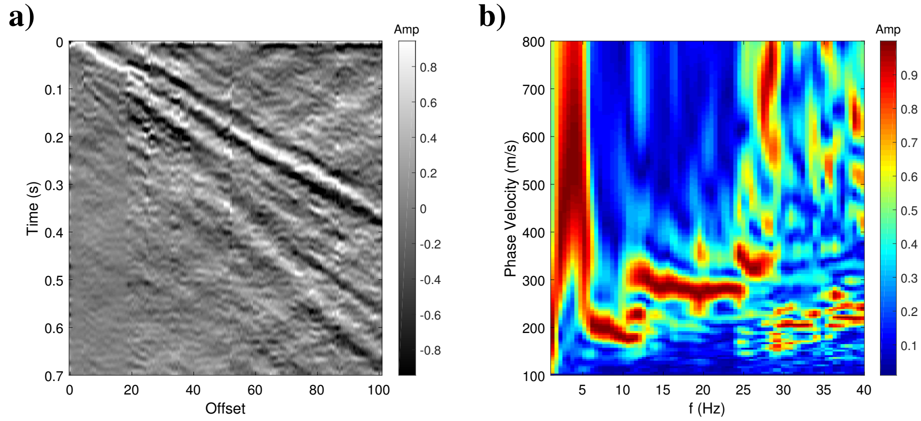

FIG. 3. (a) Virtual source gather. (b) Surface-wave dispersion spectrum.

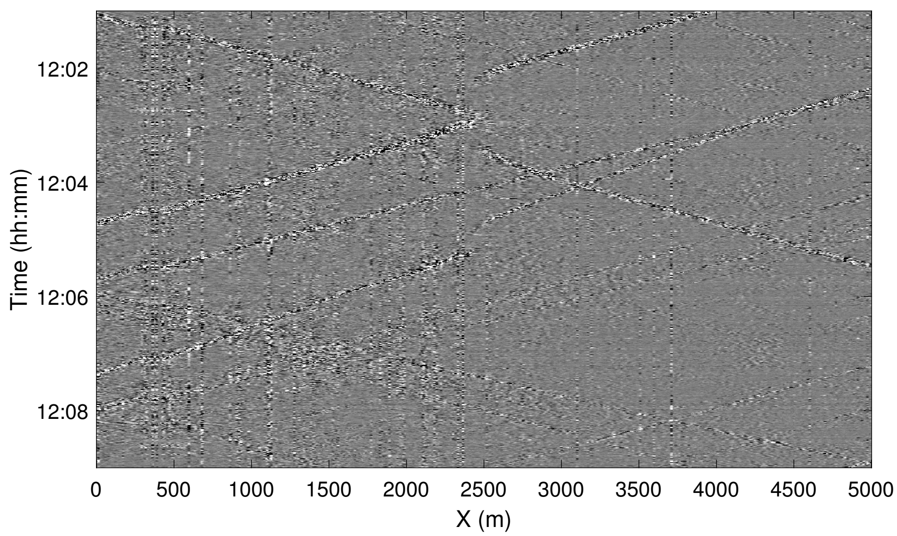

FIG. 4. Raw DAS data from the optical fibre along the Ctrain tracks.

In this part of the study, we used DAS data acquired with an optical fibre currently used for communications. The optical fibre is buried next to the tracks of the light rail transportation network of the City of Calgary, also know as the Ctrain. Due to the large volume of data available we re-sampled them at 4 ms in time and 2.0256 m in space. Figure 4 displays the data recorded for about 10 minutes along 5 km of the fibre. The large amplitude signals in Figure 4 correspond to the displacement of the Ctrain cars along the tracks. The signals propagating within the band defined by the Ctrain displacement propagate at very large velocities (> 300 m/s) as can be seen in the central part of FK spectrum in Figure 5a. We infer these signals are the result of waves propagating along the rails of the Ctrain as the cars displace. Since they do not propagate in the near-surface, but on the rails, we filter them from the data by applying a mask to their FK spectrum. The output spectrum is shown in Figure 5b. We also apply an automatic gain control using windows of 5 s to balance the amplitude of the signals present in the data. Figure 6 displays the data after denoising and amplitude balancing.

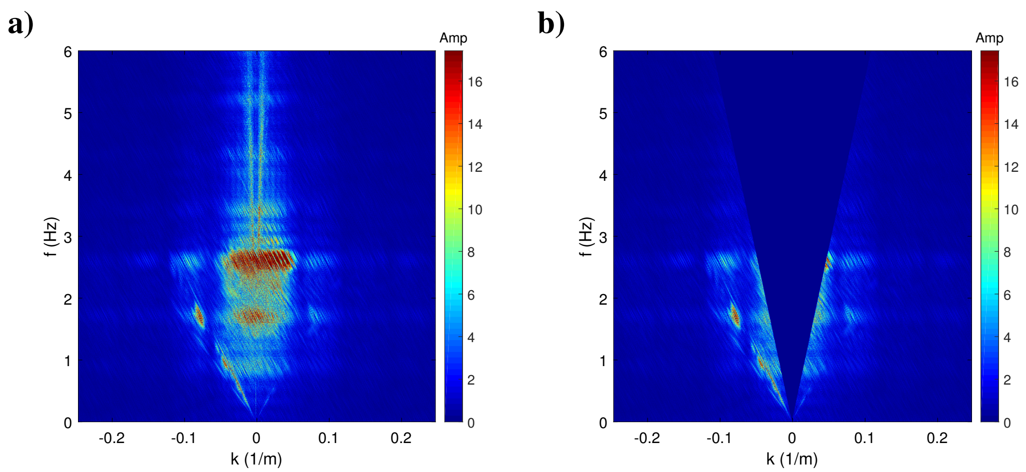

FIG. 5. FK spectra (a) before and (b) after filtering very high velocity signals (> 300 m/s).

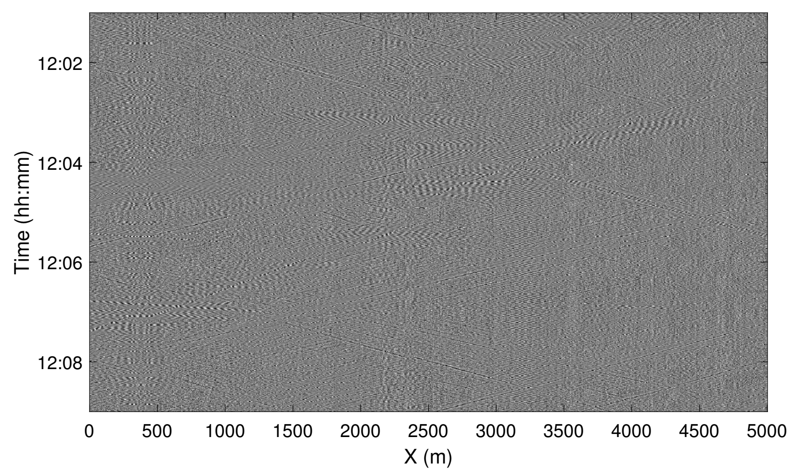

FIG. 6. DAS data after denoising and automatic gain control (agc window = 5 s).

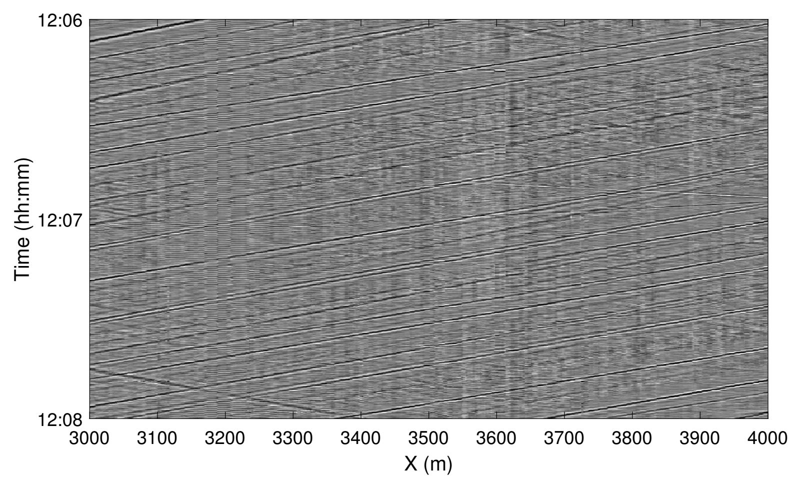

FIG. 7. Two minutes time window between $X = 3000$ m and 4000 m. All the linear events are interpreted to be the result of vehicles displacing along the road.

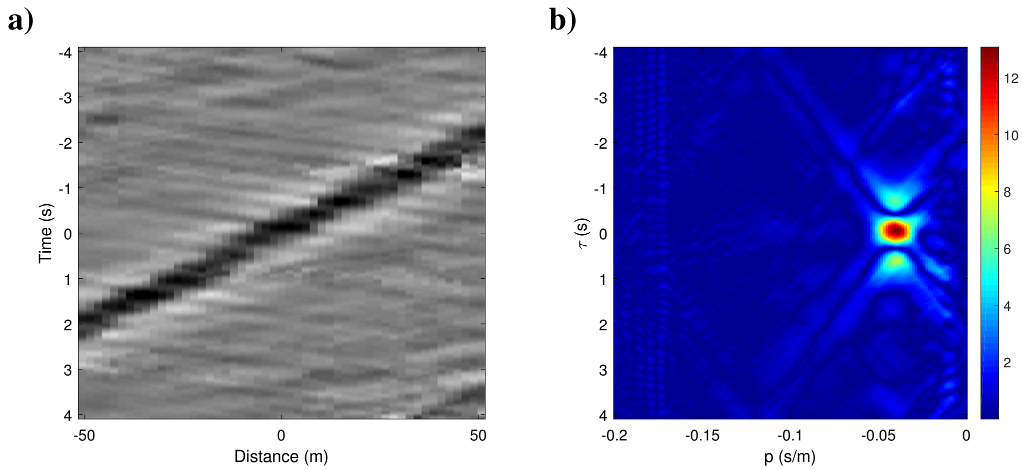

FIG. 8. (a) Example of data window and (b) the absolute value of its corresponding τ-p transformation. The p value corresponding to the maximum energy of the τ-p transform represents the slowness (1/velocity) of the linear event in (a).

To better illustrate the character of the events present in the data in Figure 7 we show the data contained in a window of 2 minutes between the X-locations at 3000 m and 4000 m. There we can see a series of linear events most of them propagating from right to left, i.e. from north to south given the orientation of the fibre. Other events with opposite slope, but with less energy, can also be observed in the data. We interpret these coherent linear events as the signature of vehicles propagating in the highway parallel to the Ctrain tracks. Therefore, the slope of these events represent the apparent velocity of the vehicles as they displace on the road.

We then computed the velocity of the linear events on Figure 7 by windowing the data in subsets of 100 m and 8 s (Figure 8a) and performing a τ-p transformation over these data (Figure 8b). The τ-p transform consists of a series of summations over a range of straight lines defined as,

$$U(\tau, p) = \int d(x, \tau - px)dx, \tag{1}$$

where $d(x, \tau - px)$ is the data along a straight line with slope p and intersect time τ and $U(\tau, p)$ is the τ-p representation of the data.

We then extracted the slowness p corresponding to the maximum energy of the τ-p slice intersecting the center of the window. The slowness p was then transformed to velocity by taking its inverse, this corresponds to the velocity of the linear event captured in the window. In Figure 8b, we can observe how the linear event in Figure 8a is focused with maximum energy around $\tau = 0$ s. This maximum occurs for a p value of -0.041 s/m which corresponds to a velocity of 24.4 m/s (87.8 km/h).

We also extracted the maximum amplitude of the slice and use it as an indicator of the strength of any captured linear event. Data windows with high-amplitude linear events will produce a large amplitude value at their corresponding velocity. In contrast, data windows with no linear events will result in τ-p transformations with very low energy. Figure 9a shows the maximum amplitude of the τ-p transformations computed over the data in Figure

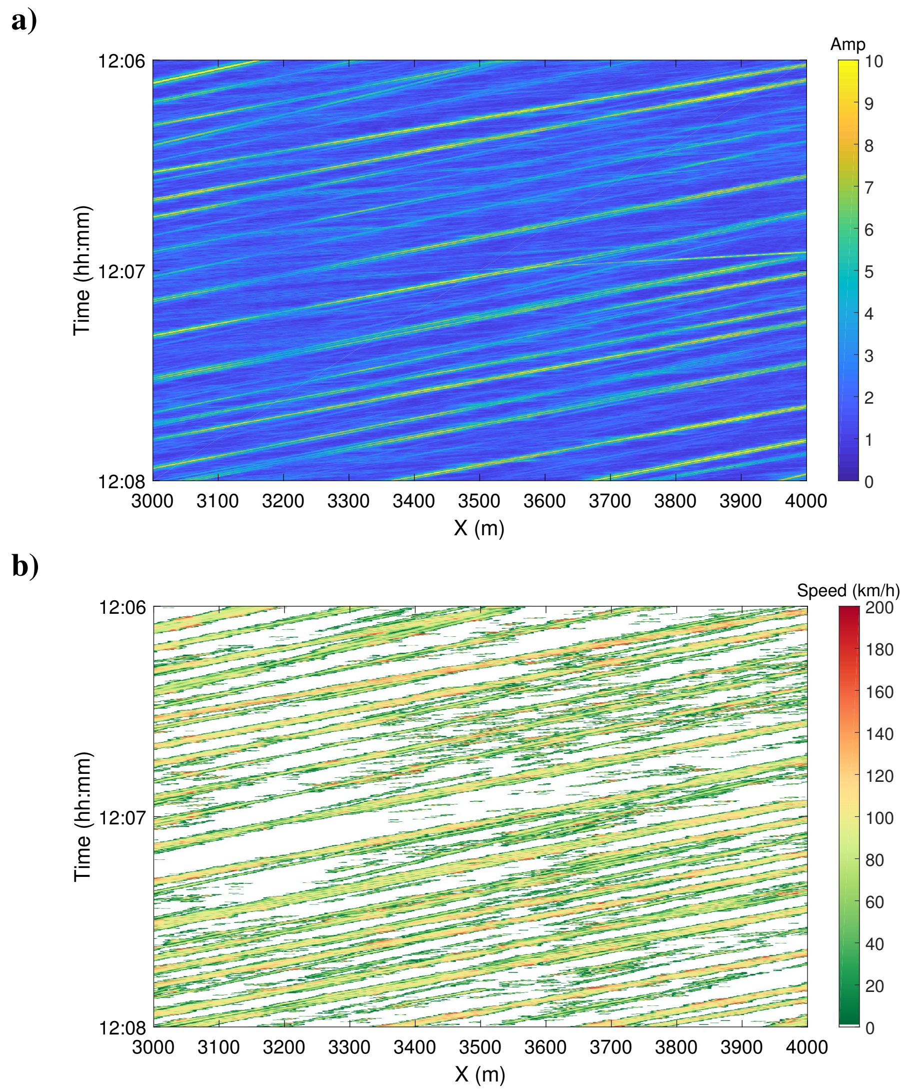

FIG. 9. (a) τ-p energy and (b) apparent velocity of the linear events in Figure 7.

7. There, we only performed τ-p transformations using negative p values in order to isolate events travelling in only one direction. Figure 9b displays the velocities of the events captured by the τ-p transformations. We only include the velocities of data points where the τ-p amplitudes are larger than 2. This plot allows us to track the speed of any vehicle along a given segment of the road in a given period of time.

We then extended the velocity extraction process to the rest of the data (Figure 10). From there, we computed three additional metrics. First, in Figure 11a we present the number of vehicles per minute detected at each location along the fibre. We computed this metric by counting the number of signals with velocities larger than zero in 1-minute windows. Second, we computed the average velocity (Figure 11b) using the same data windows. Finally, we computed the estimated total time it would take a vehicle to travel along the 5 km of the fibre (Figure 11c). This was done by simply integrating the average slowness map along the spatial axis. These plots allow us to understand the traffic flow at any given time of the day and at any segment of the road. No significant trends were iden-

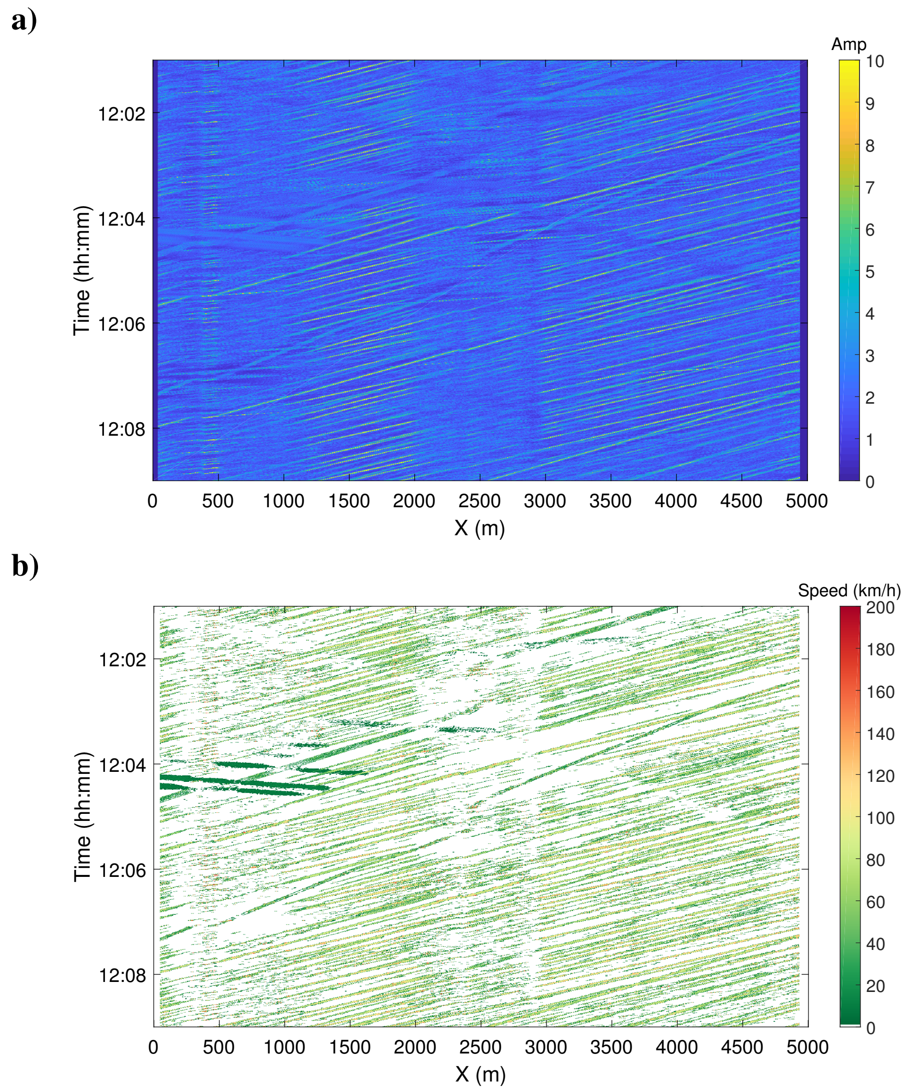

FIG. 10. (a) τ-p energy and (b) apparent velocity of the linear events in Figure 6. The dark areas around t = 12:04 and between 0 and 2500 m are the results of aliasing remaining after the FK filtering.

tified in the 10 minutes of data that were analyzed. The application of the processing here explained to a large dataset spanning several hours and even days remains to be explored.

CONCLUSIONS

The top tens of meters of the subsurface serve as the foundation of most of the infrastructure around cities. For this reason, it is important to monitor changes in the near-surface and ensure they do not result in hazardous conditions for the infrastructure that it supports. Since changes in the physical conditions of the near-surface sediments will result in changes in their elastic parameters, seismic monitoring is a tool that can provide early warnings of near-surface hazards.

We showed how DAS data can be used to compute surface-wave dispersion spectra with a very inexpensive source effort. Dispersion curves can be extracted from this spectra

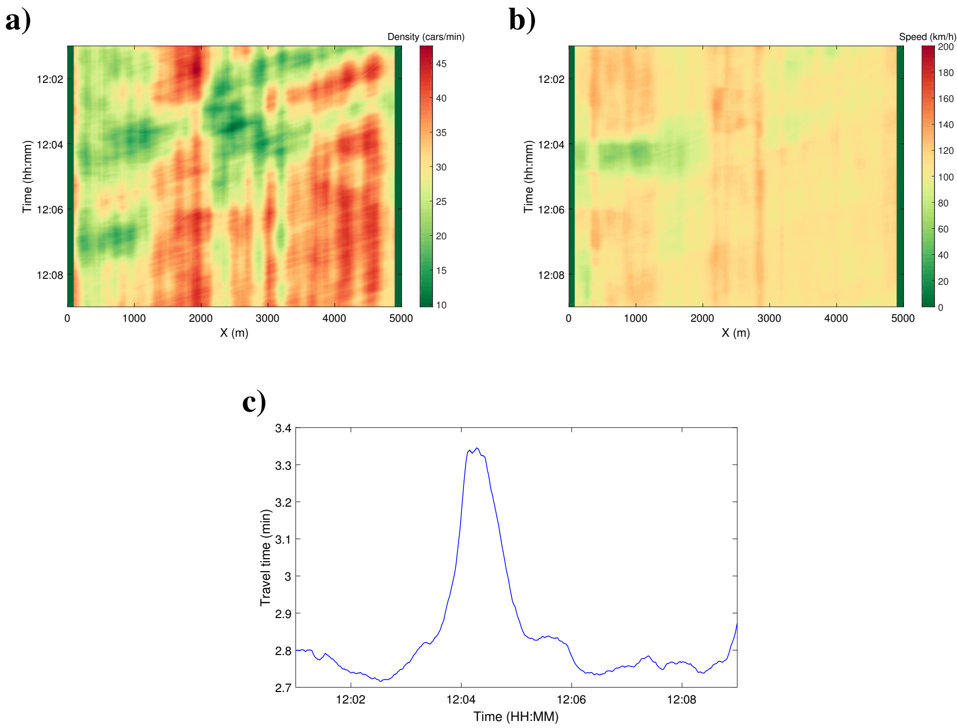

FIG. 11. (a) Approximate number of linear events per minute. (b) Average speed computed over 1-minute windows. (c) Estimated total time to complete the 5 km travel along the fibre.

and input into a S-wave velocity inversion algorithm. The very dense character of the DAS measurements allows to reduce the spatial aliasing characteristic of most surface-wave data acquisitions. Furthermore, the permanent and continuous nature of the DAS data allow to repeat this experiment multiple times over long periods of time. By continuously computing S-wave velocity models, it is possible to detect changes in the sediments in the near-surface over time. Most of the processing used in this study requires very limited human intervention. This sets the stage for the development of automatic near-surface monitoring and early warning systems based on DAS measurements.

We also explored an application of the DAS data for intelligent transportation systems. In this realm, DAS measurements can also provide a cost-effective option for continuous monitoring of roads over large distances. More importantly, buried optical fibres offer high resistance to temperature, corrosion, and electromagnetic interference rendering their maintenance a very low-cost operation. Here, we used DAS data to compute the average velocity, vehicles density, and total travel time along a segment of 5 km of an optical fibre. Computing these parameters over large period of times can help to reveal transit flow patterns. These data can be critical for taking road management decisions oriented toward an efficient use of existing roads and the planning of future ones.

With the advances and growth in the number of self-driving vehicles on the roads, real-time DAS measurement can provide complementary data to the on-board sensors of this type of vehicles. In this case, DAS measurements can help to improve drivers safety by providing data under any weather and visibility conditions where the on-board sensors are challenged.

All the results presented in this study are exploratory and they need to be validated by comparing them with other sources of data. In particular, we think that the combination of DAS data with video monitoring tools can help to calibrate the DAS measurements. Moreover, the combination of video captures with the signals registered by the optical fibre can help to design artificial intelligence algorithms able to discriminate different types of vehicles. This could provide one more degree of discrimination in the metrics for traffic flow, allowing us to study the traffic patterns of light and heavy vehicles independently.

ACKNOWLEDGEMENTS

The authors thank the sponsors of CREWES for continued support and the Pacific Institute for the Mathematical Sciences (PIMS) for organizing the Industrial Problem Solving Workshop 2018. We are also grateful to Fotech Solutions for providing the data used in this study. This work was funded by CREWES industrial sponsors, CFREF (Canada First Research Excellence Fund) and NSERC (Natural Science and Engineering Research Council of Canada) through the grant CRDPJ 461179-13. Da Li thanks the China Scholarship Council (CSC) for supporting the research.

REFERENCES

Barbagli, B., Manes, G., and Facchini, R., 2012, Acoustic sensor network for vehicle traffic monitoring: VEHICULAR 2012: International Conference on Advances in Vehicular Systems, Technologies and Applications, 1–6.

Bensen, G. D., Ritzwoller, M. H., Barmin, M. P., Levshin, A. L., Lin, F., Moschetti, M. P., Shapiro, N. M., and Yang, Y., 2007, Processing seismic ambient noise data to obtain reliable broad-band surface wave dispersion measurements: Geophysical Journal International, **169**, No. 3, 1239–1260.

Claerbout, J. F., 1968, Synthesis of a layered medium from its acoustic transmission response: Geophysics, **33**, No. 2, 264–269.

Dou, S., Lindsey, N., Wagner, A. M., Daley, T. M., Freifeld, B., Robertson, M., Peterson, J., Ulrich, C., Martin, E. R., Ajo-Franklin, J. B., and et al., 2017, Distributed acoustic sensing for seismic monitoring of the near surface: A traffic-noise interferometry case study: Scientific Reports, **7**, No. 1.

Lobkis, O. I., and Weaver, R. L., 2001, On the emergence of the Green's function in the correlations of a diffuse field: The Journal of the Acoustical Society of America, **110**, No. 6, 3011–3017.

Park, C. B., Miller, R. D., and Xia, J., 1999, Multichannel analysis of surface waves: Geophysics, **64**, No. 3, 800–808.

Schuster, G. T., Yu, J., Sheng, J., and Rickett, J., 2004, Interferometric/daylight seismic imaging: Geophysical Journal International, **157**, No. 2, 838–852.

Shapiro, N. M., and Campillo, M., 2004, Emergence of broadband Rayleigh waves from correlations of the ambient seismic noise: Geophysical Research Letters, **31**, No. 7.

Wapenaar, K., 2004, Retrieving the elastodynamic Green's function of an arbitrary inhomogeneous medium by cross correlation: Physical Review Letters, **93**, 254,301.1–254,301.4.

Zeng, X., Lancelle, C., Thurber, C., Fratta, D., Wang, H., Lord, N., Chalari, A., and Clarke, A., 2017, Properties of noise cross-correlation functions obtained from a DAS array at Garner Valley, California: Bulletin of the Seismological Society of America, **107**, No. 2, 603.